

International Journal of Modern Physics E  
© World Scientific Publishing Company

## Superfluidity of $\Lambda$ hyperons in warm strange hadronic star matter

Renli Xu

*Key Laboratory of Modern Acoustics and Department of Physics,  
Nanjing University, Nanjing 210093, P. R. China  
xurenli.phy@gmail.com*

Chen Wu

*Shanghai Institute of Applied Physics, Chinese Academy of Sciences,  
Shanghai 201800, P. R. China  
wuchenoffd@gmail.com*

Zhongzhou Ren

*Key Laboratory of Modern Acoustics and Department of Physics,  
Nanjing University, Nanjing 210093, P. R. China  
Center of Theoretical Nuclear Physics, National Laboratory of Heavy-Ion Accelerator,  
Lanzhou 730000, P. R. China  
Joint Center of Nuclear Science and Technology,  
Nanjing University, Nanjing 210093, P. R. China  
zren@nju.edu.cn*

Received 15 May 2014

Accepted 22 October 2014

In this work we evaluate the  $^1S_0$  superfluidity of  $\Lambda$  hyperons in  $\beta$ -stable strange hadronic matter. We investigate the equation of state (EOS) of hadronic matter at finite values of baryon density and temperature in the relativistic mean field (RMF) theory. Effects of the introduced isoscalar-isovector cross-interaction term on the  $\Lambda$  superfluidity are investigated systematically. In addition, the temperature effects on the superfluidity of  $\Lambda$  hyperons in hadronic matter are discussed. It is found that the density region and the magnitude of the  $\Lambda$  pairing gap are dependent on the cross-interaction term. The obtained maximal critical temperature of  $\Lambda$  superfluid is around  $10^9$  K.

*Keywords:* Nuclear matter;  $\Lambda$  hyperons; Superfluidity; Energy gap function.

PACS number(s): 26.60.-c, 21.30.Fe, 26.60.Kp

### 1. Introduction

The nuclear physics of hadronic matter has become a hot topic that connects astrophysics with extreme high-density nuclear physics.<sup>1–11</sup> With the progress of astronomical observation and nuclear experiment, astrophysics phenomena and nuclear physics are combined more and more tightly. Meantime, neutron star matters have also been attracting much interest because they offer a good chance of studying

the occurrence of superfluidity in nuclear matter.<sup>12–18</sup> Superfluidity of baryons in hadronic star matters is expected to have a number of consequences directly related to observational effects, such as cooling rates and the glitches in rotational rates that are observed in a number of pulsars.<sup>19–21</sup> It is well believed that baryon superfluidity plays an incisive role in the thermal evolution of neutron stars.<sup>22–24</sup> Baryon pairing may significantly suppress cooling rates that rely on neutrino emission from the direct Urca process.<sup>25–27</sup>

In the neutron star interior, hyperons are possible to appear through the weak interaction with the fast rise of the baryon density. Generally,  $\Lambda$  particle, the lightest hyperon with an attractive potential, is the first hyperon appearing in nuclear matter.<sup>28–30</sup> The  $^1S_0$   $\Lambda$  superfluid may occur in nuclear medium due to the attractive  $\Lambda\Lambda$  interaction.<sup>31–34</sup> Over the last decade, there have been several literatures about the nucleon and hyperon superfluidity in hadronic matter. In the work of Alm *et al.*,<sup>13</sup> the superfluid  $^3D_2$  proton-neutron pairing in dense isospin-asymmetric nuclear matter is investigated in terms of the real-time Green functions approach. They found that the critical temperature associated with the transition to the superfluid phase becomes strongly suppressed with increasing isospin asymmetry. In Ref. 27, Balberg and Barnea studied the  $^1S_0$  gap energies of  $\Lambda$  hyperons in neutron star matter, using the  $G$ -matrix effective interaction. They found that a gap energy of several tenths of a MeV is expected for a  $\Lambda$  Fermi momenta,  $k_F(\Lambda)$ , below  $1.3 \text{ fm}^{-1}$ . In Refs. 31, 33 and 34, Takatsuka and Tamagaki investigated superfluidity of  $\Lambda$  hyperons by a realistic approach using bare  $\Lambda\Lambda$  interactions and the effective mass of  $\Lambda$  based on the  $G$ -matrix calculations. Their calculation predicts  $\Lambda$  superfluid can exist in a density region between  $2\rho_0$  and  $(3–4.5)\rho_0$ ,<sup>31</sup> depending on hyperon core models. Besides, the predicted critical temperature of  $\Lambda$  superfluidity is around  $10^9$  K in hyperon-mixed neutron star cores.<sup>33</sup> Tanigawa *et al.* have investigated the  $\Lambda\Lambda$  pairing in binary mixed matter of nucleons and  $\Lambda$  hyperons, using the relativistic Hartree-Bogoliubov model combined with the relativistic mean field (RMF) interaction in Ref. 32. Therein, it is found that the value of the  $\Lambda\Lambda$  pairing gap decreases as the background nucleon density increases. In the work of Wang and Shen,<sup>28</sup> the  $^1S_0$   $\Lambda$  superfluidity in neutron star matter and neutron stars has been investigated by employing several  $\Lambda\Lambda$  interactions based on the Nijmegen models. It is found that the maximal pairing gap obtained is a few tenths of a MeV, and the magnitude and the density region of the pairing gap are dependent on the  $\Lambda\Lambda$  interaction.

In this work, we focus on the temperature effects on the  $^1S_0$  superfluidity of  $\Lambda$  hyperons in strange hadronic matter by means of the RMF model with the inclusion of the full octet of baryons. The RMF is a pioneering framework to describe the nuclear system as a relativistic many-body system of baryons and mesons, which has been widely used to investigate the properties of finite nuclei and nuclear matter.<sup>35–46</sup> Along this direction, many important extensions of RMF theory have been made, for example, the additional isoscalar-isovector cross-interaction term was introduced into the extended RMF model recently.<sup>40–42</sup> The additional

isoscalar-isovector coupling term is proved to play an important role in softening the symmetry energy at high densities and reducing the neutron skin thickness in heavy nuclei. In this work, we will systematically investigate the influence of the isoscalar-isovector coupling term on the superfluidity of  $\Lambda$  hyperons. Furthermore, we investigate the temperature effects on the  $\Lambda$  superfluidity in nuclear medium in terms of RMF model for the first time. In our calculation, we firstly investigate the equation of state (EOS) of strange hadronic matter at finite values of baryon density and temperature, then solve the finite-temperature gap equation to discuss the  $\Lambda$  superfluid in hadronic matter.

The organization of this paper is as follows. In Sec. 2, we outline the theoretical framework of the RMF theory for the hadronic matter at finite temperature. In Sec. 3, we briefly describe the energy gap equation for  $\Lambda$  hyperon pairing. The model parameters are discussed in Sec. 4. In Sec. 5, numerical results and discussions are presented. Finally, the main conclusions are summarized in Sec. 6.

## 2. Formulas of the RMF model

In the RMF theory, the nuclear interaction is usually described by the exchange of three mesons: the isoscalar meson  $\sigma$  which produces the medium range attraction, the isoscalar-vector meson  $\omega$  responsible for the short range repulsion, and the isovector-vector meson  $\rho$  reproducing the correct value of the empirical symmetry energy.<sup>47</sup> Here, the cross-interaction term  $\omega^2\rho^2$  is included, which was introduced to soften the symmetry energy at high densities.<sup>40</sup> The baryons considered in this work include the full octet of the lightest ones ( $N(p, n)$ ,  $\Lambda$ ,  $\Sigma^+$ ,  $\Sigma^0$ ,  $\Sigma^-$ ,  $\Xi^0$ ,  $\Xi^-$ ) originally investigated by Glendenning.<sup>48</sup> The total Lagrangian density  $\mathcal{L}$  takes the form

$$\begin{aligned} \mathcal{L} = & \sum_j \bar{\psi}_j [i\gamma^\mu \partial_\mu - M_j + g_{\sigma j} \sigma - g_{\omega j} \gamma^\mu \omega_\mu - \frac{g_{\rho j}}{2} \gamma^\mu \tau \cdot \rho_\mu] \psi_j + \frac{1}{2} \partial^\mu \sigma \partial_\mu \sigma \\ & - \frac{1}{2} m_\sigma^2 \sigma^2 - \frac{1}{4} \Omega^{\mu\nu} \Omega_{\mu\nu} + \frac{1}{2} m_\omega^2 \omega^\mu \omega_\mu - \frac{1}{4} G^{\mu\nu} G_{\mu\nu} + \frac{1}{2} m_\rho^2 \rho^\mu \rho_\mu \\ & - U_{eff}(\sigma, \omega^\mu, \rho^\mu) + \sum_l \bar{\psi}_l [i\gamma^\mu \partial_\mu - m_l] \psi_l, \end{aligned} \quad (1)$$

where the index  $j$  runs over the full octet of baryons, and  $l$  represents electrons and muons ( $e$  and  $\mu$ ).  $M_j$  denotes the vacuum baryon mass of index  $j$ . The antisymmetric tensors of the vector mesons are taken as the usual forms  $\Omega_{\mu\nu} = \partial_\mu \omega_\nu - \partial_\nu \omega_\mu$  and  $G_{\mu\nu} = \partial_\mu \rho_\nu - \partial_\nu \rho_\mu$ .  $g_{\sigma j}$ ,  $g_{\omega j}$  and  $g_{\rho j}$  are the coupling constants between the baryon and  $\sigma$  meson,  $\omega$  meson, and  $\rho$  meson, respectively. The nonlinear self-interacting terms of  $\sigma$ ,  $\omega$  and the isoscalar-isovector cross-interaction are taken as

$$\begin{aligned} U_{eff}(\sigma, \omega^\mu, \rho^\mu) = & \frac{\kappa}{3!} (g_{\sigma N} \sigma)^3 + \frac{\lambda}{4!} (g_{\sigma N} \sigma)^4 - \frac{\zeta}{4!} (g_{\omega N}^2 \omega_\mu \omega^\mu)^2 \\ & - \Lambda_v (g_{\rho N}^2 \rho_\mu \rho^\mu) (g_{\omega N}^2 \omega_\mu \omega^\mu). \end{aligned} \quad (2)$$

4 *R.L. Xu, C. Wu, and Z. Z. Ren*

By virtue of translational and rotational invariance, the meson fields are constant in infinite nuclear matter. As a consequence, the field equations under the mean-field approximation have the following form

$$(i\gamma^\mu\partial_\mu - M_j^* - g_{\omega j}\gamma^0\omega - \frac{g_{\rho j}}{2}\gamma^0\tau_{3j}\rho)\psi_j = 0, \quad (3)$$

$$m_\sigma^2\sigma + \frac{\kappa}{2}g_{\sigma N}^3\sigma^2 + \frac{\lambda}{6}g_{\sigma N}^4\sigma^3 = \sum_i g_{\sigma i}\rho_i^S, \quad (4)$$

$$m_\omega^2\omega + \frac{\zeta}{6}g_{\omega N}^4\omega^3 + 2\Lambda_\nu g_{\rho N}^2 g_{\omega N}^2 \rho^2\omega = \sum_i g_{\omega i}\rho_i^B, \quad (5)$$

$$m_\rho^2\rho + 2\Lambda_\nu g_{\rho N}^2 g_{\omega N}^2 \omega^2\rho = \sum_i \frac{g_{\rho i}}{2}\tau_{3i}\rho_i^B. \quad (6)$$

The effective mass of baryon octet, in equation (3), is given as

$$M_j^* = M_j - g_{\sigma j}\sigma. \quad (7)$$

$\rho_i^S$  and  $\rho_i^B$  are the baryon scalar density and the baryon density of the particle symbolled by  $i$ , respectively. They are written as

$$\rho_i^S = \frac{2}{(2\pi)^3} \int d^3k \frac{M_i^*}{\sqrt{k^2 + M_i^{*2}}} [f_i(k) + \bar{f}_i(k)], \quad (8)$$

$$\rho_i^B = \frac{2}{(2\pi)^3} \int d^3k [f_i(k) - \bar{f}_i(k)], \quad (9)$$

where  $f_i(k)$  and  $\bar{f}_i(k)$  are the fermion particle distribution and antiparticle distribution:

$$f_i(k) = \frac{1}{\exp\{(\sqrt{k^2 + M_i^{*2}} - \nu_i)/T\} + 1}, \quad (10)$$

$$\bar{f}_i(k) = \frac{1}{\exp\{(\sqrt{k^2 + M_i^{*2}} + \nu_i)/T\} + 1}, \quad (11)$$

with  $\nu_i$  being the effective chemical potential, related to the chemical potential  $\mu_i$  as

$$\nu_i = \mu_i - g_{\omega i}\omega - g_{\rho i}\tau_{3i}\rho. \quad (12)$$

For the hadronic matter with baryons and charged leptons, the  $\beta$ -equilibrium conditions under the weak processes are given by

$$\mu_p = \mu_{\Sigma^+} = \mu_n - \mu_e, \quad (13)$$

$$\mu_\Lambda = \mu_{\Sigma^0} = \mu_{\Xi^0} = \mu_n, \quad (14)$$

$$\mu_{\Sigma^-} = \mu_{\Xi^-} = \mu_n + \mu_e, \quad (15)$$

$$\mu_\mu = \mu_e, \quad (16)$$

and the charge neutrality condition is fulfilled by

$$\rho_p + \rho_{\Sigma^+} = \rho_{\Sigma^-} + \rho_{\Xi^-} + \rho_e + \rho_\mu, \quad (17)$$

where  $\rho_i$  is the number density of particle  $i$ . At a given baryon density  $\rho_B$  and a given temperature  $T$ , the Dirac equation (3) can be solved exactly with plane waves as solutions, while the coupled eqs. (4)–(6) and (13)–(17) can be solved self-consistently. Once the solution has been found, the EOS of the hadronic matter can be calculated from

$$\begin{aligned} \epsilon = & \sum_i \frac{2}{(2\pi)^3} \int d^3k \sqrt{k^2 + m_i^{*2}} [f_i(k) + \bar{f}_i(k)] + \frac{1}{2} m_\sigma^2 \sigma^2 + \frac{\kappa}{6} g_{\sigma N}^3 \sigma^3 \\ & + \frac{\lambda}{24} g_{\sigma N}^4 \sigma^4 + \frac{1}{2} m_\omega^2 \omega^2 + \frac{\xi}{8} g_{\omega N}^4 \omega^4 + \frac{1}{2} m_\rho^2 \rho^2 + 3\Lambda_\nu g_{\rho N}^2 g_{\omega N}^2 \omega^2 \rho^2 \\ & + \frac{1}{\pi^2} \sum_l \int k^2 \sqrt{k^2 + m_l^2} [f_l(k) + \bar{f}_l(k)] dk, \end{aligned} \quad (18)$$

$$\begin{aligned} p = & \sum_i \frac{1}{3} \frac{2}{(2\pi)^3} \int d^3k \frac{k^2}{\sqrt{k^2 + m_i^{*2}}} [f_i(k) + \bar{f}_i(k)] - \frac{1}{2} m_\sigma^2 \sigma^2 - \frac{\kappa}{6} g_{\sigma N}^3 \sigma^3 \\ & - \frac{\lambda}{24} g_{\sigma N}^4 \sigma^4 + \frac{1}{2} m_\omega^2 \omega^2 + \frac{\xi}{24} g_{\omega N}^4 \omega^4 + \frac{1}{2} m_\rho^2 \rho^2 + \Lambda_\nu g_{\rho N}^2 g_{\omega N}^2 \omega^2 \rho^2 \\ & + \frac{1}{3\pi^2} \sum_l \int \frac{k^4}{\sqrt{k^2 + m_l^2}} [f_l(k) + \bar{f}_l(k)] dk. \end{aligned} \quad (19)$$

Meanwhile, the single-particle energy for the  $\Lambda$  hyperons, and the  $\Lambda$  chemical potential at a given baryon density  $\rho_B$  can also be obtained, which are crucial in the investigation on the superfluidity of  $\Lambda$  hyperons.

### 3. Energy gap equation for $\Lambda$ hyperon pairing

In this work, we investigate the  $^1S_0$  superfluidity of  $\Lambda$  hyperons in warm strange hadronic matter. As a key quantity to determine the onset of superfluidity, the energy gap function  $\Delta_k$  can be obtained by solving the finite-temperature gap equation

$$\Delta_k = -\frac{1}{\pi} \int k'^2 dk' V(k, k') \frac{\Delta_{k'}}{E_{k'}} \tanh\left(\frac{E_{k'}}{2T}\right), \quad (20)$$

$$E_{k'} = \sqrt{[\varepsilon(k') - \mu_\Lambda]^2 + \Delta_{k'}^2}, \quad (21)$$

where  $\varepsilon(k')$  is the single-particle energy in the nuclear medium for the  $\Lambda$  hyperons,  $\mu_\Lambda$  the corresponding chemical potential at a given baryon density  $\rho_B$ . The single-particle energy of  $\Lambda$  hyperons in the RMF approach is written as

$$\varepsilon(k) = \sqrt{k^2 + m_\Lambda^{*2}} + g_{\omega\Lambda} \omega \quad (22)$$

The potential matrix element for the  $^1S_0$   $\Lambda$  pairing interaction can be given by

$$V(k, k') = \langle k | V_{\Lambda\Lambda}(^1S_0) | k' \rangle = \int r^2 dr j_0(kr) V_{\Lambda\Lambda}(r) j_0(k'r), \quad (23)$$

6 *R.L. Xu, C. Wu, and Z. Z. Ren*

where  $j_0(kr) = \sin(kr)/(kr)$  is the zero order spherical Bessel function.  $V_{\Lambda\Lambda}(r)$  is the  $^1S_0$   $\Lambda$  pairing interaction potential in coordinate space. It is known that the magnitude of the pairing gap are influenced by the  $\Lambda\Lambda$  interaction. Here, we adopt the ND1, ND2, ESC00, NSC97b, NSC97e and NSC97f potentials obtained by fitting to the corresponding Nijmegen models,<sup>49–51</sup> as well as the NFs and NSC97s potentials obtained by reproducing the  $\Lambda\Lambda$  binding energy value of  $B_{\Lambda\Lambda}(^6_{\Lambda\Lambda}\text{He})$  from the Nagara event.<sup>52</sup> To solve the gap equation, we follow the separation method developed by Khodel *et al.*<sup>53</sup>

#### 4. Model parameters

To examine the influence of the isoscalar-isovector cross-interaction on the superfluidity of  $\Lambda$  hyperons, we employ the parameter set FSU in the present calculation, meanwhile, the parameter sets NL3 and NL3\* are also included for comparison. As for the meson-hyperon couplings, the values in the SU(6) quark model are taken for the vector coupling constants

$$\begin{aligned} g_{\omega\Lambda} &= g_{\omega\Sigma} = 2g_{\omega\Xi} = \frac{2}{3}g_{\omega N}, \\ g_{\rho\Lambda} &= 0, \quad g_{\rho\Sigma} = 2g_{\rho\Xi} = 2g_{\rho N}. \end{aligned} \quad (24)$$

The scalar coupling constant of  $\Lambda$  hyperons is chosen to fit the  $\Lambda$  hypernuclei observables so as to reproduce the descriptions of  $\Lambda$  hypernuclei and  $\Lambda$  hyperons in nuclear matter self-consistently. Studying for the  $\Lambda$  hypernuclei with FSU, NL3, and NL3\*, in Ref. 54, we obtained the relative  $\sigma$  coupling for  $\Lambda$  as  $R_{\sigma\Lambda}=0.619$  for the FSU,  $R_{\sigma\Lambda}=0.620$  for the NL3\* and  $R_{\sigma\Lambda}=0.621$  for the NL3 parameter set. The  $R_{\sigma\Lambda}$  is defined as  $R_{\sigma\Lambda} = g_{\sigma\Lambda}/g_{\sigma N}$ . With these scalar couplings, we obtain the potential depth of a  $\Lambda$  in saturated nuclear matter as:  $U_{\Lambda}^{(N)} = -29.99$  MeV for FSU,  $U_{\Lambda}^{(N)} = -30.31$  MeV for NL3\* and  $U_{\Lambda}^{(N)} = -30.42$  MeV for NL3, which are all close to the reasonable  $\Lambda$  hyperon potential  $U_{\Lambda}^{(N)} \simeq -30$  MeV.<sup>3</sup> For  $\Sigma$  hyperons, The study of  $\Sigma^-$  atoms showed strong evidence for a sizable repulsive potential in the nuclear core.<sup>55,56</sup> A recent work again confirmed the repulsive nature of the  $\Sigma^-$  potential with a new geometric analysis of the  $\Sigma^-$  atom data.<sup>57</sup> Therefore, for the  $\Sigma$ - $N$  interaction, we adopt  $U_{\Sigma}^{(N)} = 30$  MeV as used in Ref. 3 to determine the scalar coupling constants. Besides, for the  $\Xi$ - $N$  interaction, we take the potential  $U_{\Xi}^{(N)} = -15$  MeV<sup>58,59</sup> in our calculation. Then, we obtain,  $g_{\sigma\Sigma} = 4.717$  and  $g_{\sigma\Xi} = 3.161$  for the NL3 parameter set,  $g_{\sigma\Sigma} = 4.650$  and  $g_{\sigma\Xi} = 3.119$  for the NL3\* parameter set, and  $g_{\sigma\Sigma} = 4.820$  and  $g_{\sigma\Xi} = 3.279$  for the FSU parameter set, respectively.

For systematically investigate the influence of the isoscalar-isovector cross-interaction on the superfluidity of  $\Lambda$  hyperons, we change the  $\Lambda_{\nu}$  in our calculation. For a given  $\Lambda_{\nu}$ , we follow Refs. 60,61 and 62 to readjust the  $\rho NN$  coupling constant  $g_{\rho}$  so as to keep the symmetry energy unchanged at  $k_F = 1.15$  fm<sup>-1</sup>. This simple procedure produces a nearly constant binding energy per nucleon for <sup>208</sup>Pb as  $\Lambda_{\nu}$  is

Table 1. Readjusted parameters in NL3\* and FSU. The binding energy per nucleon ( $E/A$ ), proton radius ( $r_p$ ), and neutron skin thickness ( $r_n - r_p$ ) for  $^{208}\text{Pb}$  are listed.

model	$\Lambda_\nu$	$g_\rho$	$E/A$ (MeV)	$r_p$ (fm)	$r_n - r_p$ (fm)
FSUw1	0.01	9.6550	-7.866	5.461	0.259
FSUw2	0.02	10.5558	-7.871	5.466	0.233
FSU	0.03	11.7673	-7.873	5.473	0.206
FSUw4	0.04	13.5221	-7.868	5.482	0.175
NL3*w1	0.01	9.8047	-7.882	5.452	0.256
NL3*w2	0.02	10.6242	-7.896	5.456	0.226
NL3*w3	0.03	11.6909	-7.903	5.463	0.196
NL3*w4	0.04	13.1605	-7.905	5.472	0.164

changed.<sup>60</sup> The readjusted parameters with various  $\Lambda_\nu$  are listed in Table 1, where the parameter sets are named according to the value of  $\Lambda_\nu$ , except for the original parameter sets FSU.

## 5. Numerical results and discussion

In this section, we study the  $^1S_0$   $\Lambda$  superfluidity in warm strange hadronic matter. Firstly, for investigating the influence of the isoscalar-isovector cross-interaction on the superfluidity of  $\Lambda$  hyperons, we show the energy gap  $\Delta_F$  of the  $\Lambda$  hyperons in hadronic matter at  $T = 0$  with several parameter sets in Fig. 1. Where, the  $\Delta_F$  is the energy gap of  $\Lambda$  hyperons at the Fermi surface. Considering the computing time, here, we just use the ESC00 potential for example. As we see in Fig. 1, The

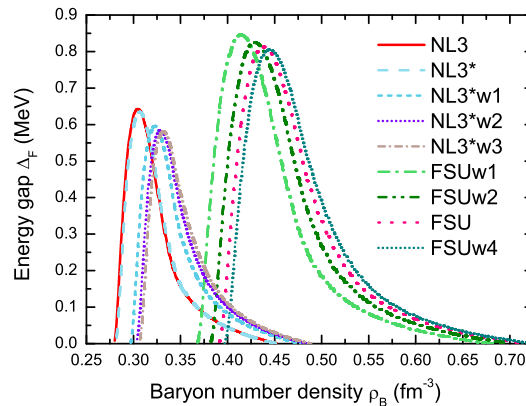


Fig. 1. Density dependence of the  $^1S_0$   $\Lambda$  energy gap  $\Delta_F$  in  $\beta$ -stable hadronic matter at  $T = 0$  with NL3, NL3\* and FSU, as well as the readjusted parameters in NL3\* and FSU. The used  $\Lambda\Lambda$  interaction is ESC00 potential.

threshold density of  $\Lambda$  is around  $0.39 \text{ fm}^{-3}$  calculated with FSU. In the case of FSU, a  $^1S_0$   $\Lambda$  superfluid is formed as soon as the  $\Lambda$  hyperons appear in hadronic matter. Besides, the same result can also be obtained for the other eight parameter sets in our calculation. It is found that the maximal energy gap  $\Delta_F$  of  $\Lambda$  with the ESC00 potential for the case of FSU is about 0.81 MeV, while the result is about 0.63 MeV for both NL3\* and NL3, which is in accord with the result in Ref. 28. Additionally, in Fig. 1, we find that the maximal energy gap gradually becomes smaller as the nonlinear coupling  $\Lambda_\nu$  increases for both the NL3\* and FSU. Besides, the baryon density corresponding to the maximal energy gap increases with the nonlinear coupling  $\Lambda_\nu$  for NL3\* and FSU, respectively.

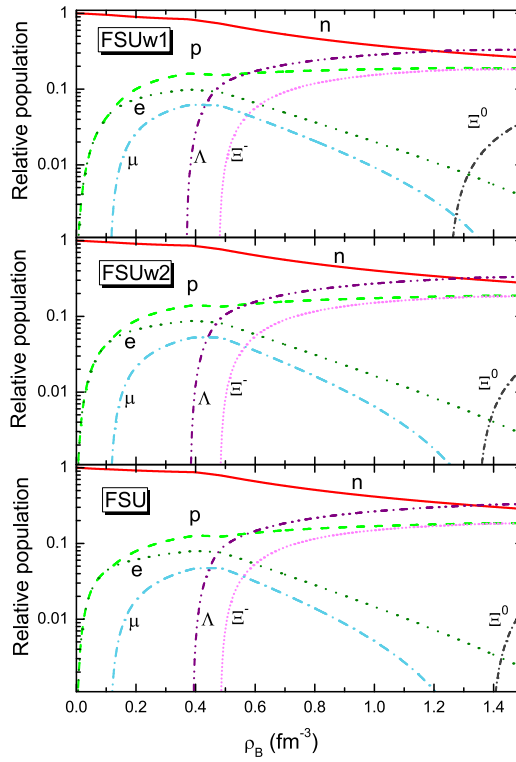


Fig. 2. Calculated variation behavior of the relative populations of the compositions of hadronic matter with respect to the total baryon density  $\rho_B$  at  $T=0$  in FSUw1, FSUw2 and FSU, respectively.

For the properties of  $\Lambda$  hyperons in nuclear medium also play an important role on the  $\Lambda$  energy gap, in Fig. 2, we depict the relative populations of all compositions with respect to the total baryon density at  $T = 0$ . Here, we take the results

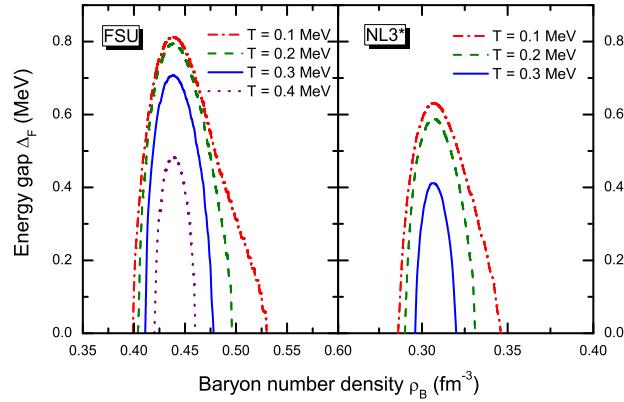


Fig. 3. Density dependence of the  $^1S_0$   $\Lambda$  energy gap  $\Delta_F$  in  $\beta$ -stable hadronic matter with FSU at  $T=0.1, 0.2, 0.3$  and  $0.4$  MeV, and with NL3\* at  $T=0.1, 0.2$  and  $0.3$  MeV. The used  $\Lambda\Lambda$  interaction is ESC00 potential.

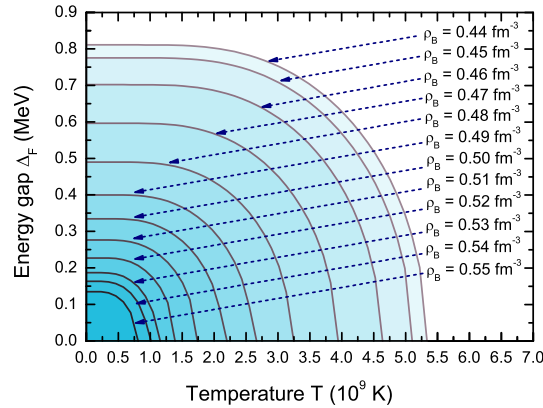


Fig. 4. Temperature dependence of the  $^1S_0$   $\Lambda$  energy gap  $\Delta_F$  in  $\beta$ -stable hadronic matter with FSU. The baryon density  $\rho_B$  ranges from  $0.44 \text{ fm}^{-3}$  to  $0.55 \text{ fm}^{-3}$ . The used  $\Lambda\Lambda$  interaction is ESC00 potential.

with FSUw1, FSUw2 and FSU for example. For the  $\Lambda$  hyperons, their relative populations increase rapidly with the ascent of the density near the onset region of  $\Lambda$  hyperons, then they increase very slowly with the increase of the baryon density at higher density. The results show that the threshold density of  $\Lambda$  increases with the nonlinear coupling  $\Lambda_\nu$  increasing. As shown in Fig. 2, the cross-interaction may have an important influence on the properties of  $\Xi^0$  hyperons in nuclear medium, which needs more discussion in future work.

Table 2. The critical temperature of  $^1S_0$   $\Lambda$  superfluid at different baryon densities. The quantities  $Y$  and  $\Delta_F$  represent the fraction of  $\Lambda$  hyperon ( $Y = \rho_\Lambda/\rho_B$ ) and the  $^1S_0$   $\Lambda$  energy gap in  $\beta$ -stable hadronic matter.  $T_c^{cal.}$  and  $T_c^{WCA}$  are the calculated critical temperature with ESC00 potential in the case of FSU and the corresponding weak-coupling approximation (WCA) estimations.

$\rho_B$ (fm $^{-3}$ )	$Y$	$\Delta_F$ (MeV)	$T_c^{cal.}$ ( $10^9$ K)	$T_c^{WCA}$ ( $10^9$ K)
0.41	1.25%	0.502	3.36	3.33
0.42	2.14%	0.697	4.64	4.61
0.43	3.08%	0.791	5.22	5.23
0.44	4.06%	0.810	5.34	5.36
0.45	5.06%	0.775	5.11	5.13
0.46	6.06%	0.702	4.64	4.65
0.47	7.06%	0.597	3.94	3.95
0.48	8.05%	0.490	3.25	3.24
0.49	8.85%	0.400	2.67	2.65
0.50	9.50%	0.335	2.20	2.22
0.51	10.10%	0.271	1.74	1.79
0.52	10.67%	0.223	1.39	1.47
0.53	11.22%	0.182	1.16	1.20
0.54	11.75%	0.163	1.01	1.08
0.55	12.26%	0.135	0.81	0.89

In order to investigate the temperature dependence of the superfluidity of  $\Lambda$  hyperons, in Fig. 3, we show the energy gap  $\Delta_F$  of the  $\Lambda$  hyperons in hadronic matter in FSU, and NL3\* included for comparison. For both of the two parameter sets, with the temperature increasing, the maximal energy gap of  $\Lambda$  pairing decreases, besides, the onset density of  $\Lambda$  superfluidity becomes higher and the density where  $\Lambda$  superfluidity disappear becomes lower. However, the density corresponding to the maximal energy gap is almost unchanged with the temperature increasing, which is about  $0.44 \text{ fm}^{-3}$  in the case of FSU and about  $0.31 \text{ fm}^{-3}$  in NL3\*. For better understanding, in Fig. 4, we show the temperature dependence of the energy gap  $\Delta_F$  of  $\Lambda$  for several values of the total baryon number density in FSU for example. Fig. 4 is obtained with the range of the temperature  $T$  from 0 to 0.48 MeV, with the steps being 0.01 MeV. Finally it should be pointed out that the finite-temperature gap equation solution is a very lengthy calculation. It takes more than 600 CPU hours with one processor. As shown in Fig. 4, the energy gaps of  $\Lambda$  at different baryon density are almost unchanged in low temperature region, then they decrease rapidly with the increase of the temperature and disappear at some critical temperature.

In Table 2, we list the  $\beta$ -stable fractions of the  $\Lambda$  and the critical temperature, as well as the estimated result from the well-known weak-coupling approximation (WCA).<sup>63</sup>

$$T_c \approx 0.57\Delta_F(T = 0). \quad (25)$$

As seen in Table 2, the calculated critical temperature of the  $^1S_0$   $\Lambda$  superfluid is in good agreement with the WCA. In our case of FSU, the fractions of the  $\Lambda$

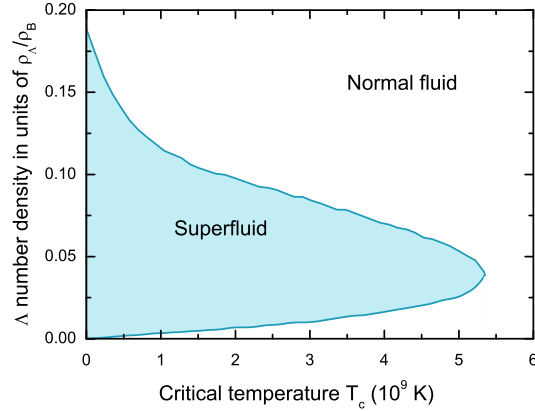


Fig. 5. Critical temperature of the  $^1S_0$   $\Lambda$  superfluid as a function of the  $\Lambda$  number density in units of  $\rho_\Lambda/\rho_B$  calculated with FSU parameter set. The used  $\Lambda\Lambda$  interaction is ESC00 potential.

Table 3. Maximal pairing gap  $\Delta_F$  at Fermi surface and the critical temperature of  $^1S_0$   $\Lambda$  superfluid obtained with several  $\Lambda\Lambda$  potentials.  $\rho_B$  is the total baryon density of  $\beta$ -stable hadronic matter corresponding to the maximal pairing gap, and  $T_c^{cal.}$  is the calculated critical temperature. The used parameter sets are FSU and NL3\*.

	FSU			NL3*		
	$\rho_B$ ( $\text{fm}^{-3}$ )	$\Delta_F$ (MeV)	$T_c^{cal.}$ ( $10^9$ K)	$\rho_B$ ( $\text{fm}^{-3}$ )	$\Delta_F$ (MeV)	$T_c^{cal.}$ ( $10^9$ K)
ESC00	0.439	0.81	5.34	0.306	0.63	4.19
ND1	0.432	0.18	1.16	0.304	0.14	0.92
ND2	0.429	0.12	0.73	0.301	$9.8 \times 10^{-2}$	0.65
NSC97b	0.402	$2.0 \times 10^{-3}$	$1.3 \times 10^{-2}$	0.286	$1.7 \times 10^{-3}$	$1.1 \times 10^{-2}$
NSC97e	0.406	$4.3 \times 10^{-3}$	$2.7 \times 10^{-2}$	0.289	$3.7 \times 10^{-3}$	$2.3 \times 10^{-2}$
NSC97f	0.400	$1.7 \times 10^{-3}$	$1.0 \times 10^{-2}$	0.286	$1.4 \times 10^{-3}$	$8.8 \times 10^{-3}$
NSC97s	0.414	$1.1 \times 10^{-2}$	$6.7 \times 10^{-2}$	0.293	$9.9 \times 10^{-3}$	$5.6 \times 10^{-2}$
NFs	0.432	$1.7 \times 10^{-2}$	0.10	0.304	$1.5 \times 10^{-2}$	0.09

in warm hadronic matter, corresponding to the maximal critical temperature, is about 4%. Then, with the fractions of the  $\Lambda$  increasing, the corresponding critical temperature decreases. When the fractions of the  $\Lambda$  approaches to 19%, there will be no  $^1S_0$   $\Lambda$  superfluid any more in our calculation. In addition, our calculation about the maximal energy gap  $\Delta_F$  of  $\Lambda$  as well as the corresponding fractions of the  $\Lambda$  are in accord with the result obtained by using the G-matrix effective interaction in Ref. 27, where they found that a maximum gap energy of 0.8–0.9 MeV is achieved for a  $\Lambda$  fraction of about 5%.

In Fig. 5, we show the region in the temperature- $\Lambda$ -density plane where the  $\Lambda$  hyperon is expected to be superfluid. In the case of FSU, the  $\Lambda$  is in a  $^1S_0$

superfluid state for fractions of the  $\Lambda$  ranging from  $3.8 \times 10^{-3} \%$  up to  $\sim 18.8\%$ , which corresponds to a total baryon density ranging from the  $\Lambda$  onset density  $0.39 \text{ fm}^{-3}$  to  $\sim 0.71 \text{ fm}^{-3}$  at  $T = 0$ . With the temperature increasing, the density region for  $\Lambda$  superfluid becomes narrow. As seen in Fig. 5, the  $^1S_0$   $\Lambda$  superfluid only exists when the stellar matter cools down to about  $5.4 \times 10^9$  K. Above this maximal critical temperature of  $\Lambda$  superfluid, there still may exist  $^1S_0$   $\Sigma^-$  pairing and  $^3P_2$  neutron pairing.<sup>64</sup>

Finally, we list the maximal pairing gap ( $\Delta_F$ ) at the Fermi surface and the critical temperature obtained with several  $\Lambda\Lambda$  potentials in Table 3. The total baryon density corresponding to the maximal pairing gap calculated with FSU is around  $0.4 \text{ fm}^{-3}$  with these  $\Lambda\Lambda$  potentials, while it is around  $0.3 \text{ fm}^{-3}$  in the case of NL3\*. However, the maximal pairing gap  $\Delta_F$  and the critical temperature predicted with FSU and NL3\* are similar to each other. Additionally, the critical temperature of  $^1S_0$   $\Lambda$  superfluid is around  $10^7$  K with the NSC97s and NFs potentials in the case of FSU and NL3\*.

## 6. Summary

In this article, the  $^1S_0$  superfluidity of  $\Lambda$  hyperons in warm strange hadronic matter, in  $\beta$  equilibrium by including the full octet of baryons, is investigated within the RMF models. By changing the strength of the isoscalar-isovector cross-interaction in RMF models (NL3\* and FSU), we systematically investigate the influence of the cross-interaction term on the properties of  $^1S_0$   $\Lambda$  superfluid. It is found that with the isoscalar-isovector coupling increasing, the onset density and the density corresponding to the maximal energy gap of  $^1S_0$   $\Lambda$  superfluid increases. However, the maximal energy gap of  $\Lambda$  pairings gradually becomes smaller with the isoscalar-isovector coupling. In addition, it is found that the maximal energy gap  $\Delta_F$  of  $\Lambda$  in  $\beta$ -stable hadronic matter at  $T = 0$  is about 0.81 (0.63) MeV with the ESC00 potential in the case of FSU (NL3\*). The value of  $\Delta_F$  is 0.1 – 0.2 MeV for the ND1 and ND2 potentials. The NSC97b, NSC97e, NSC97f, NSC97s and NFs potentials reproduce the value of  $\Delta_F$  of the order of  $10^{-3} - 10^{-2}$  MeV.

On the other hand, with the temperature increasing, the onset density of  $^1S_0$   $\Lambda$  superfluid becomes higher and the disappearance density becomes lower, while the density corresponding to the maximal energy gap is almost unchanged. The energy gaps of  $\Lambda$  pairing at different baryon density are almost unchanged in low temperature region, then they decrease rapidly with the increase of the temperature and disappear at some critical temperature. The maximal critical temperature of  $\Lambda$  superfluid is about  $5.3$  ( $4.2$ )  $\times 10^9$  K in the case of FSU (NL3\*) with the ESC00 potential. The maximal critical temperature of  $\Lambda$  superfluid is of the order of  $10^7 - 10^9$  K with the ND1, ND2, NSC97b, NSC97e, NSC97f, NSC97s and NFs potentials.

## Acknowledgements

The authors would like to thank the anonymous referee for her/his constructive suggestions which are very helpful to improve this manuscript. This work was supported by the National Natural Science Foundation of China (Grants No. 11035001, No. 11375086, No. 10735010, No. 10975072, No. 11120101005, No. 11175232 and No. 11105072), by the 973 National Major State Basic Research and Development of China (Grants No. 2013CB834400, No. 2014CB845402 and No. 2010CB327803), by CAS Knowledge Innovation Project No. KJCX2-SW-N02, by Research Fund of Doctoral Point (Grant No. 20100091110028), by the Project Funded by the Priority Academic Program Development of Jiangsu Higher Education Institutions (PAPD), and by the Research and Innovation Project for College Postgraduate of JiangSu Province, Grants No. KYZZ\_0023.

## References

1. J. Schaffner *et al.*, *Phys. Rev. Lett.* **71** (1993) 1328.
2. H. Müller and B.D. Serot, *Nucl. Phys. A* **606** (1996) 508.
3. J. Schaffner-Bielich and A. Gal, *Phys. Rev. C* **62** (2000) 034311.
4. J.E. Trümper, *Prog. Part. Nucl. Phys.* **66** (2011) 674.
5. A. Akmal, V.R. Pandharipande and D.G. Ravenhall, *Phys. Rev. C* **58** (1998) 1804.
6. J. Schaffner and I.N. Mishustin, *Phys. Rev. C* **53** (1996) 1416.
7. S. Typel and H.H. Wolter, *Nucl. Phys. A* **656** (1999) 331.
8. T. Klähn *et al.*, *Phys. Rev. C* **74** (2006) 035802.
9. A. Lavagno, *Phys. Rev. C* **81** (2010) 044909.
10. P.K. Panda, C. Providência and D.P. Menezes, *Phys. Rev. C* **82** (2010) 045801.
11. H. Shen, H. Toki, K. Oyamatsu and K. Sumiyoshi, *Nucl. Phys. A* **637** (1998) 435.
12. H. Kucharek and P. Ring, *Z. Phys. A* **339** (1991) 23.
13. T. Alm, G. Röpke, A. Sedrakian and F. Weber, *Nucl. Phys. A* **604** (1996) 491.
14. N. Sandulescu, *Phys. Rev. C* **70** (2004) 025801.
15. M. Baldo, U. Lombardo, E.E. Saperstein and S.V. Tolokonnikov, *Nucl. Phys. A* **750** (2005) 409.
16. R. Aguirre, *Phys. Rev. C* **85** (2012) 064314.
17. I. Bombaci and U. Lombardo, *Phys. Rev. C* **44** (1991) 1892.
18. X.R. Zhou, H.-J. Schulze, F. Pan and J.P. Draayer, *Phys. Rev. Lett.* **95** (2005) 051101.
19. C.J. Pethick and D.G. Ravenhall, *Annu. Rev. Nucl. Part. Sci.* **45** (1995) 429.
20. D. Pines and M.A. Alpar, *Nature* **316** (1985) 27.
21. M.A. Alpar, H.F. Chau, K.S. Cheng and D. Pines, *Astrophys. J.* **409** (1993) 345.
22. D. Page, M. Prakash, J.M. Lattimer and A.W. Steiner, *Phys. Rev. Lett.* **85** (2000) 2048.
23. H. Heiselberg and M. Hjorth-Jensen, *Phys. Rep.* **328** (2000) 237.
24. D.J. Dean and M. Hjorth-Jensen, *Rev. Mod. Phys.* **75** (2003) 607.
25. S. Tsuruta, *et al.*, *Astrophys. J.* **691** (2009) 621.
26. T. Takatsuka, S. Nishizaki, Y. Yamamoto and R. Tamagaki, *Prog. Theor. Phys.* **115** (2006) 355.
27. S. Balberg and N. Barnea, *Phys. Rev. C* **57** (1998) 409.
28. Y.N. Wang and H. Shen, *Phys. Rev. C* **81** (2010) 025801.
29. N.K. Glendenning, *Phys. Rev. C* **64** (2001) 025801.
30. P.K. Panda, D.P. Menezes and C. Providencia, *Phys. Rev. C* **69** (2004) 025207.

- 14 R.L. Xu, C. Wu, and Z. Z. Ren
31. T. Takatsuka and R. Tamagaki, *Nucl. Phys. A* **670** (2000) 222c.  
32. T. Tanigawa, M. Matsuzaki and S. Chiba, *Phys. Rev. C* **68** (2003) 015801.  
33. T. Takatsuka and R. Tamagaki, *Nucl. Phys. A* **721** (2003) 1003c.  
34. T. Takatsuka and R. Tamagaki, *Prog. Theor. Phys.* **102** (1999) 1043.  
35. P. Ring, *Prog. Part. Nucl. Phys.* **37** (1996) 193.  
36. P. Ring, *Prog. Part. Nucl. Phys.* **46** (2001) 165.  
37. G.A. Lalazissis, J. König and P. Ring, *Phys. Rev. C* **55** (1997) 540.  
38. G.A. Lalazissis and P. Ring, *Phys. Lett. B* **427** (1998) 225.  
39. G.A. Lalazissis, et al., *Phys. Lett. B* **671** (2009) 36.  
40. B.G. Todd-Rutel and J. Piekarewicz, *Phys. Rev. Lett.* **95** (2005) 122501.  
41. J. Piekarewicz, *Phys. Rev. C* **73** (2006) 044325.  
42. F.J. Fattoyev, C.J. Horowitz, J. Piekarewicz and G. Shen, *Phys. Rev. C* **82** (2010) 055803.  
43. B.K. Agrawal, A. Sulaksono and P.G. Reinhard, *Nucl. Phys. A* **882** (2012) 1.  
44. Z.Z. Ren, A. Faessler and A. Bobyk, *Phys. Rev. C* **57** (1998) 2752.  
45. Z.Z. Ren, F. Tai and D.H. Chen, *Phys. Rev. C* **66** (2002) 064306.  
46. C. Wu and Z.Z. Ren, *Phys. Rev. C* **83** (2011) 025805.  
47. B.D. Serot and J.D. Walecka, *Phys. Lett. B* **87** (1979) 172.  
48. N.K. Glendenning, *Phys. Lett. B* **114** (1982) 392.  
49. E. Hiyama, M. Kamimura, T. Motoba, T. Yamada and Y. Yamamoto, *Prog. Theor. Phys.* **97** (1997) 881.  
50. T.A. Rijken, *Nucl. Phys. A* **691** (2001) 322c.  
51. I.N. Filikhin and A. Gal, *Nucl. Phys. A* **707** (2002) 491.  
52. H. Takahashi *et al.*, *Phys. Rev. Lett.* **87** (2001) 212502.  
53. V.A. Khodel, V.V. Khodel and J.W. Clark, *Nucl. Phys. A* **598** (1996) 390.  
54. R.L. Xu, C. Wu and Z.Z. Ren, *J. Phys. G: Nucl. Part. Phys.* **39** (2012) 085107.  
55. C.J. Batty, E. Friedman and A. Gal, *Phys. Lett. B* **335** (1994) 273.  
56. J. Mareš, E. Friedman, A. Gal and B.K. Jennings, *Nucl. Phys. A* **594** (1995) 311.  
57. E. Friedman and A. Gal, *Phys. Rep.* **452** (2007) 89.  
58. P. Khaustov *et al.*, *Phys. Rev. C* **61** (2000) 054603.  
59. C. Ishizuka, A. Ohnishi, K. Tsubakihara, K. Sumiyoshi and S. Yamada, *J. Phys. G: Nucl. Part. Phys.* **35** (2008) 085201.  
60. C.J. Horowitz and J. Piekarewicz, *Phys. Rev. Lett.* **86** (2001) 5647.  
61. W.Z. Jiang, *Phys. Rev. C* **81** (2010) 044306.  
62. R. Cavagnoli, D.P. Menezes and C. Providência, *Phys. Rev. C* **84** (2011) 065810.  
63. E.M. Lifshitz and L.P. Pitaevskii, *Statistical Physics Part 2* (Pergamon, Oxford, 1980).  
64. I. Vidaña and L. Tolós, *Phys. Rev. C* **70** (2004) 028802.

## BIB<sub>T</sub>E<sub>X</sub>ing in IJMPE BIBStyle

### 1. Usage

```
\documentclass{ws-ijmpe}
\usepackage{url}
\begin{document}
Sample output using ws-ijmpe bibliography style file ...
...text.\cite{best,pier,jame} ...
\bibliographystyle{ws-ijmpe}
\bibliography{sample}
\end{document}
```

### 2. Output

Sample output using ws-ijmpe bibliography style file

- (1) article: ...text.<sup>?,?,?,?</sup>
- (2) proceedings: ...text.<sup>?</sup>
- (3) inproceedings: ...text.<sup>?,?</sup>
- (4) book: ...text.<sup>?</sup>
- (5) edition: ...text.<sup>?</sup>
- (6) editor: ...text.<sup>?</sup>
- (7) series: ...text.<sup>?</sup>
- (8) tech report: ...text.<sup>?,?</sup>
- (9) unpublished: ...text.<sup>?,?,?</sup>
- (10) phd thesis: ...text.<sup>?</sup>
- (11) masters thesis: ...text.<sup>?</sup>
- (12) incollection: ...text.<sup>?</sup>
- (13) booklet: ...text.<sup>?</sup>
- (14) misc: When the reference forms part of the sentence, it should not be typed in superscripts, e.g.: “One can show from Ref. ? that ...”